Journal of
Ceramic Science
and Technology

*J. Ceram. Sci. Tech.*, **06** [03] 237-244 (2015)
DOI: 10.4416/JCST2014-00058
available online at: http://www.ceramic-science.com


# Highly Porous Scaffolds Made of Nanosized Hydroxyapatite Powder Synthesized from Eggshells

**S.M. Naga*[1], H.F. El-Maghraby[1], M. Sayed[1], E.A. Saad[2]**

[1]National Research Centre, Ceramics Department, 12622 El-Bohouth Str., Dokki, Cairo (Egypt)
[2]Ain ShamsUniversity, Faculty of Science, Chemistry Department, Cairo (Egypt)

received December 30, 2014; received in revised form January 9, 2015; accepted February 6, 2015

**Abstract**

**Nanosize hydroxyapatite powder synthesized indirectly from eggshells is used to produce 3D porous scaffolds. They are fabricated via a polymeric sponge method. X-ray diffraction (XRD) and transmission electron microscopy (TEM) are used to characterize the phase composition and grain size of the scaffolds, respectively. The results showed that the prepared powder is composed of pure hydroxyapatite with a grain size ranging between 35 and 122 nm. The prepared scaffolds calcined at 1250 °C for 2 h possess interconnected porosity (≈ 73 %). The studied scaffolds showed suitable mechanical strength necessary for bone tissue engineering. Their crushing and bending strengths were 0.82 MPa and 1.72 MPa, respectively. Thin film XRD, SEM and EDS confirmed the presence of a rich bone-like apatite layer post-immersion in SBF on the scaffold's surface.**

*Keywords: Bioceramics, hydroxyapatite, porous scaffolds, mechanical properties*

## I. Introduction

All around the world millions of tonnes of eggshells are thrown away as waste material every year from houses, restaurants, hatcheries and bakeries. Thus the utilization of eggshell waste will lead to a direct impact on both the national economy and environmental pollution of the country. According to Food and Agriculture Organization (FAO) estimation, Egypt's egg production during the period 2000 to 2012 expanded from 177 000 t to reach 310 000 t, making this country the third largest producer in the African region [1]. The eggshell represents approximately 11 % of the total weight of the egg. It is composed of calcium carbonate (94 %), magnesium carbonate (1 %), calcium phosphate (1 %), organic matter (4 %) and some trace elements such as $Mg^{2+}$, $Na^{+}$, $Sr^{2+}$ and $Si^{2+}$, which have an important role in bio-mineralization during bone formation [2–3]. Because of the natural biological origin of the eggshell, it produces hydroxyapatite (HA) having crystalline structure and composition similar to human bone [4]. Such properties have qualified eggshell for use as a promising raw material for biomedical applications.

Direct and indirect conversion methods are used to synthesize HA from eggshells [4,5]. The direct conversion process is carried out by means of hydrothermal methods [6,7]. On the other hand, the indirect process consists of two steps. In the first step, calcium precursor is prepared from the eggshell, and in the second step it is converted into HA. A number of preparation techniques have been used to synthesize HA such as, mechano-chemical, wet precipitation, sol-gel, and microwave irradiation [4,5,8,9]. Ho *et al.* [10] applied the solid state reaction technique to prepare HA. They heated the eggshell powders (used as a source of calcium) with dicalcium phosphate dihydrated (DCPD) at 1150 °C for 3 h with a heating rate of 10 °K/min.

Chaudhuri *et al.* [11] prepared nano-crystalline HA from eggshell and dipotassium phosphate ($K_2HPO_4$). They claimed that the prepared HA is very pure and it has a regular and uniform grain size. Many authors used organic modifiers such as ethylenediaminetetraacetic acid (EDTA), citric acid, and polystyrene sulfonate for the synthesis of HA. They showed that the morphology of the HA nanostructure depends on the modifier used [12–14].

Mondal *et al.* [15] prepared nano-hydroxyapatite with grain size of 78.31 nm from eggshell with the wet precipitation method. They dissolved the eggshell powder in dilute $HNO_3$ acid, then they added 0.6 M diammonium hydrogen phosphate solution dropwise with continuous stirring for 1 h.

Lee *et al.* [16] and Lee *et al.* [17] synthesized HA from calcined eggshell and phosphoric acid. Lee *et al.* [16] mixed calcined eggshell with phosphoric acid with a mixing ratio of 1.0: 1.2 CaO: phosphoric acid. They added polyethylene glycol (PEG) to the slurry to produce a finer crystallite size. They showed that the addition of PEG produced a homogeneous precursor with a grain size of 80 – 100 nm. Lee *et al.* [17] claimed that their HA powder calcined in air for 2 h possessed a grain size of 50 – 80 nm. Adak *et al.* [18] converted calcined eggshell into calcium nitrate before the reaction with ammonia and diammonium hydrogen phosphate solutions. They produced Ca-deficient HA powder with a crystallite size of 70 – 80 nm; calcination temperature was 900 °C. On the other hand, the grain size of HA powder calcined at 900 °C for 1 h synthesized by

* Corresponding author: salmanaga@yahoo.com

Prabakaran and Rajeswari [19] was 88 nm. They used the hydrothermal method and cationic surfactant cetyltrimethylammonium bromide (CTAB) as a template to synthesize nano hydroxyapatite from calcined eggshell.

Porous HA scaffolds were fabricated by means of many techniques to meet the structural and mechanical requirements of tissue engineering. Scaffolds must have a highly porous surface with highly interconnective pores. Conventional methods of porous scaffold fabrication include sponge replica, sol-gel casting methods, solvent casting/porogen leaching [20], thermally induced phase separation freeze-drying [20,22], and gas foaming/porogen leaching [23,24]. Recently, automated computer-controlled fabrication techniques like rapid prototyping (RP) have been used in biogenic scaffold preparation [25–27].

The present study aims at the fabrication of porous 3D HA scaffolds with an interconnected pore structure via the polymeric sponge method. The HA powder is prepared indirectly from eggshell powder and the physical, thermal and mechanical properties of both HA powder and scaffolds are studied. In addition, the produced HA scaffolds studied *in vitro* and mechanically evaluated. In the present study, eggshell biowaste is converted to nano-hydroxyapatite porous scaffolds that mimic the structure and biological function of natural bone with a cheap and eco-friendly method, which is, to our knowledge, a new and novel application for hydroxyapatite prepared from eggshell.

## II. Materials and Methods

### *(1) Materials*

Eggshell was collected from bakery shops, orthophosphoric acid $H_3PO_4$ (Elgoumhouria Co. for trading Medicines Ameria Cairo, Egypt), ammonia solution $NH_4OH$ (Wessex House, Shaftesbury, Dorset, UK-Molekula), polyvinyl alcohol LR (Laboratory Rasyan), distilled water, highly dense polyethylene sponge, synthetic sponge and reagent-grade NaCl, $NaHCO_3$, KCl, $Na_2HPO_4{\cdot}2H_2O$, $MgCl_2{\cdot}6H_2O$, $CaCl_2$, and $Na_2SO_4$ were used in the present study

### *(2) Methods*

#### (a) *Preparation of calcium oxide from eggshell*

The egg shell was collected, washed with distilled water, dried, then crushed and calcined at 900 °C for 2 h with heating rate of 5 °K/min in presence of an air stream to avoid carbon fixation during the calcination process. The decomposition of eggshell ($CaCO_3$) to CaO takes place according to the equation:

$$CaCO_3 \xrightarrow{900\,^{\circ}C,2h} CaO+CO_2$$

The calcined material (CaO) was stored in an airtight desiccator to minimize any possible exposure to moisture

#### (b) *Preparation of hydroxyapatite powder*

The freshly prepared CaO was mixed with the stoichiometric amount of distilled water (about 32.15 ml $H_2O$/100 g CaO) to prepare $Ca(OH)_2$, according to the equation:

$$CaO+H_2O \rightarrow Ca(OH)_2$$

0.5 M $Ca(OH)_2$ suspension and 0.3 M orthophosphoric acid were prepared with the appropriate dilutions. The 0.5 M $Ca(OH)_2$ suspension was vigorously stirred at 70 °C for 1 h, and the 0.3 M $H_3PO_4$ solution was added, at the end of the stirring time dropwise with a slow stirring rate. The pH of the solution was kept in the range 10.5 – 11 with the addition of ammonia solution. After complete addition of the $H_3PO_4$ acid solution, an additional vigorous stirring was carried out for 1 h at 70 °C. The formed slurry was left at room temperature overnight for aging. The excess ammonia solution obtained over the white precipitate powder was poured and the precipitate was washed with distilled water to remove the $NH_4^+$ ions. The precipitate was dried at 105 °C for 24 h. The HA formation reaction took place according to the following equation:

$$10Ca(OH)_2+6H_3PO_4 \rightarrow Ca_{10}(PO_4)_6(OH)_2$$

The formed powder was calcined at different firing temperatures ranging from 500 up to 1100 °C for 2 h with a heating rate of 10 °K/min. The calcined powder was finely ground completely to pass a 90-micron sieve.

#### (c) *Preparation and sintering of hydroxyapatite scaffolds*

A set of cubic and rectangular specimens, with dimensions of 10 x 10 x 10 mm and 50 x 15 x 10 mm respectively, were cut from pieces of high-density polyethylene sponge. Specimens were immersed in the HA slurry under vacuum for 3 h to form porous HA scaffolds by firing. The soaked samples were dried slowly at 50 °C for 6 h, then at 80 °C for 6 h and finally at 110 °C overnight. To accelerate the oxidation of the formed carbon produced by the sponge fiber and to sweep the gases formed, the samples were fired up to 600 °C under static air. A slow heating rate was adopted at low temperature to prevent the bodies cracking during the burnout process, i.e. a rate of 2 °K/min from room temperature to 600 °C followed by a higher rate of 5°K/min to the sintering temperature. The samples were fired at 1250 °C with a soaking time of 2 h.

#### (d) *Acellular in vitro test*

HA scaffold specimens with $10 \times 10 \times 10$ mm$^3$ were immersed in simulated body fluid (SBF) for 1, 3, 6, 12 h and 1, 3, 7, 14, 21, 28 days at 37 °C. The samples were immersed in SBF with ion concentrations nearly equal to that of human blood plasma [28] under static conditions at a concentration of approximately 0.01 g/ml of solution. 1 gm of the sample was immersed in 100 ml SBF at pH 7.4 and the temperature was kept at 37 °C during the test. After immersing process, the concentration of both calcium and phosphorus ions in the solution was analyzed. The microstructure of the immersed samples was investigated by means of SEM attached to EDS, while the formed apatite layer on the surface of scaffolds was characterized using thin-film XRD analysis.

#### (e) *Characterization*

Bulk density and apparent porosity of the fired specimens were evaluated using the Archimedes method (ASTM C-20). The phase composition of the samples was

analyzed using x-ray diffraction (XRD) using monochromated $CuK_\alpha$ radiation (D 500, Siemens, Mannheim, Germany). The microstructure of the samples was investigated by means of scanning electron microscopy (SEM; Model XL 30, Philips, Eindhoven, Netherlands). Bending strength was measured in a three-point bending test on a universal testing machine (Model 4204, Instron Corp., Danvers, MA) at a crosshead speed of 0.5 mm/min and support distance of 40 mm. At least ten specimens were measured for each data point. Mercury porosimetry (Model Poresizer 9320, Micromeritics, USA) was used to measure the samples' average pore size. The calcined HA powder was investigated with a transmission electron microscope JEOL, JEM-2100-HR, Japan to determine the grain particle size.

FTIR analysis of HA powder was carried out using a FT/IR- 6100 Fourier transform Infrared Spectrometer from JASCO, thermal analysis of the as-prepared HA powder was investigated with a Q 600 thermogravimetric analyzer (sample heated from room temperature up to 1000 °C at a heating rate of 5 °C), The crushing strength of the calcined scaffolds was measured using LR/OK plus 10 KN (2248 16 F apparatus with crosshead travel of 950 mm and speed range of 0.01 mm/min, the apparent density of HA powder was determined with a Quantachrome instrument (Corporation Upyc 1200eV 5.03). The change in the concentration of Ca and P ions was determined with an Inductively Coupled Plasma Spectrometer (ICP), Model Ultima-2, JY 2000 – 2, France, while the apatite layer formed on the surface of the immersed samples in SBF was characterized using thin-film XRD (X'Pert Pro. PANlxtical, target Cu-$K_\alpha$ with second monochromator $K\tau$=45 mA; 4, Holland).

## III. Results and Discussion

### *(1) Crude eggshell*

The XRD pattern of the crude eggshell, Fig. 1, shows that it composed completely of calcite. The characteristic peak of calcite at d = 3.03985Å is present as a sharp peak. It indicates the pronounced crystallinity of the calcite phase close to the values obtained from the JCPDS (005 – 0586) standard data. Fig. 2 reveals the porous nature of the raw eggshell. The figure shows that the calcite crystals are arranged in layers and the pores are round and homogeneously distributed in the matrix. It is indicated from Fig. 3 that the eggshell consisted of an outer porous calcareous layer, and a fibrous shell membrane.

### *(2) As-prepared and calcined HA powder*

The thermogravimetric analysis (TGA) of the as-prepared HA is shown in Fig. 4. The weight loss was observed to occur in three steps. The first step occurred between room temperature and 300 °C and is due to the evaporation of weakly entrapped water. It was found to be 5.56 %. The weight loss in the second step was found to be 0.91 %. It is observed between 300 and 500 °C. It could be due to the interstitial water during the conversion of $HPO_4^{2-}$ to $P_2O_7^{4-}$ [4,29]. The third weight loss step is observed between 500 and 1000 °C. It may be due to both the dehydroxylation and the formation of the $PO_4^{3-}$ ion in addition to the decarboxylation and the release of carbon dioxide [30].

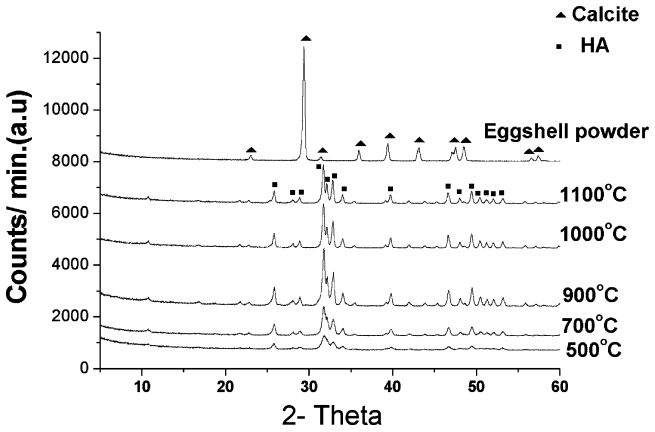


**Fig. 1:** XRD patterns of the crude eggshell and HA calcined at different firing temperatures for 2 h.

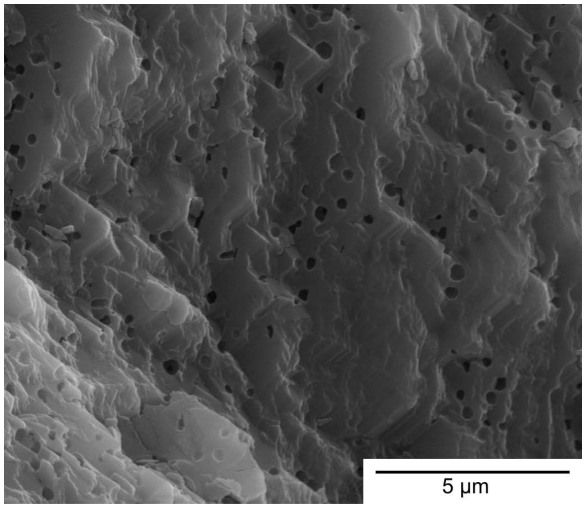


**Fig. 2:** The porous nature of the raw eggshell.

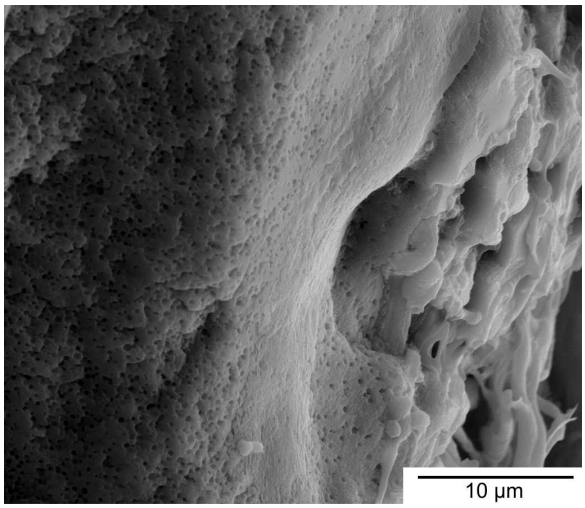


**Fig. 3:** SEM micrograph of the crude eggshell.

The as-prepared powder was calcined at 500 °, 700 °, 900 °, 1000 ° and 1100 °C for 2 h. Fig. 1 shows the XRD patterns of the calcined powders. It indicates that the powder is composed completely of HA phase. The indexed d-spacing of the samples was found to be very close to the values obtained from the JCPDS (009 – 0432) standard data. It was noticed that the intensity and sharpness of the

peaks increased with the increase in the calcination temperatures.

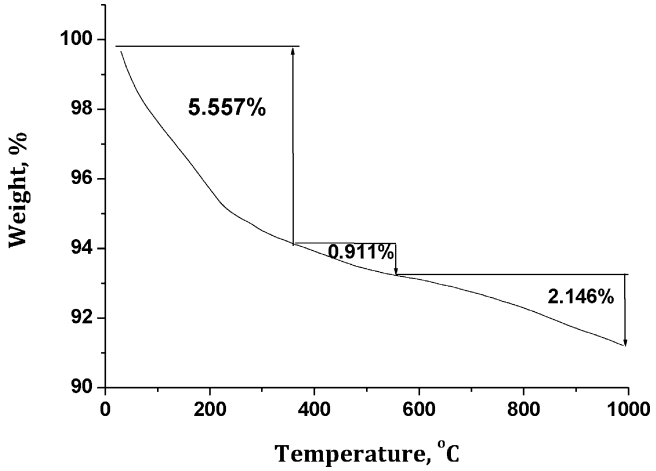


**Fig. 4:** TGA graph of the as-prepared HA powder.

The bands of the FTIR spectrum of the eggshell calcined at 900 °C are shown in Fig. 5. The spectrum shows the typical bands of HA. The absorption; bending; $\tau_4$ bands of $PO_4^{-3}$ ion appeared at 1041.37, 603.61 and 570.83 $cm^{-1}$, respectively. On the other hand, $\tau_1$ $PO_4^{-3}$ symmetrical stretching mode can be observed at 964 $cm^{-1}$. The surface hydroxyl groups of $CaHPO_4$ are detected at 3574.41 $cm^{-1}$. While the band (shoulder) that appeared at 1093.44 $cm^1$ is assigned to degenerate $\tau_3$ $PO_4^{-3}$ asymmetric stretch [30,31]. Two undefined bands were obtained at 2919.7 and 2851.24 $cm^1$.

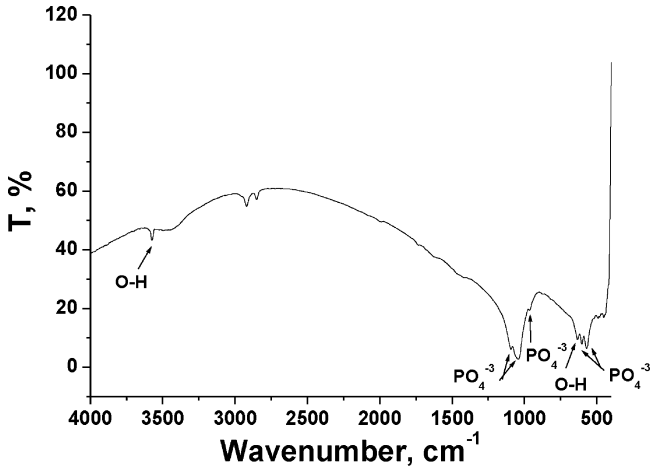


**Fig. 5:** FTIR spectrum of HA powder calcined at 900 °C for 2 h.

The TEM observations, Fig. 6, revealed that the grain size of HA powder calcined at 900 °C for 2 h ranges between 35 and 122 nm. The obtained grain size is smaller than or close to that obtained by many authors [15–19].

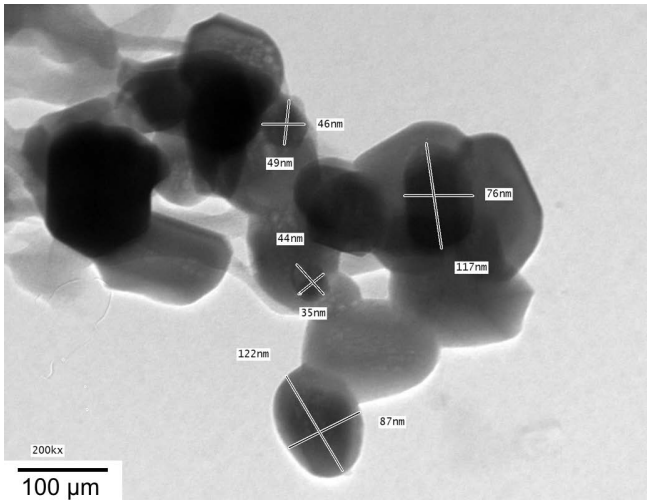


**Fig. 6:** TEM of HA powder calcined at 900 °C for 2 h.

### *(3) HA porous scaffolds*

Bone has a three-dimensional (3D) configuration; accordingly, 3D scaffolds must be used so that new tissue can be grown in a 3D manner [32]. The structure of the fabricated HA scaffold calcined at 1250 °C for 2 h is shown in Fig. 7. The figure shows rounded interconnected macropores with a diameter ranging between 20 and 420 µm. The formed pore shape and distribution maintained the initial sponge structure. It can be noticed that some of the pores seemed to be blocked, but they contain nanopores as indicated by Fig. 8. The scaffolds' pore area, median pore diameter, bulk density, bending strength, crushing strength and apparent porosity are given in Table 1. The development of an interconnected pore structure is an essential feature for the bio-scaffolds. They enhance the implant attachment by allowing the new bone tissue infiltration. Kim and Mooney [32] showed that biocompatible scaffolds should have high porosity with an interconnected pore network for cell growth and flow transport of nutrients and metabolic wastes. The apparent porosity of the calcined scaffolds is 73 % with a median pore diameter of 41.72 µm. We believe that the calcined HA scaffolds satisfy the requirements for biocompatible scaffolds.

**Table 1:** Pore area, median pore diameter, bulk density, apparent porosity, bending strength, and crushing strength of calcined HA scaffolds.

| Pore area, $m^2/g$ | Median pore diameter, µm | Bulk density, $g/cm^3$ | Apparent porosity, % | Bending strength, MPa | Crushing strength, MPa |
|---|---|---|---|---|---|
| 3.76 | 41.72 | 0.98 ± 0.11 | 73 ± 1.9 | 1.72 ± 0.11 | 0.82 ± 0.01 |

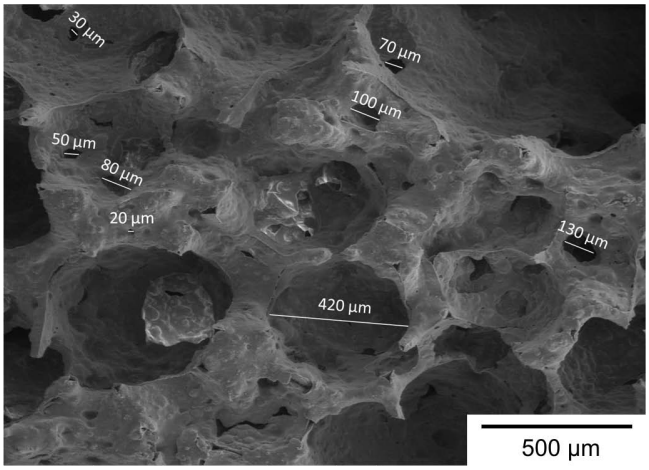


**Fig. 7:** SEM of the HA scaffold calcined at 1250 °C for 2 h.

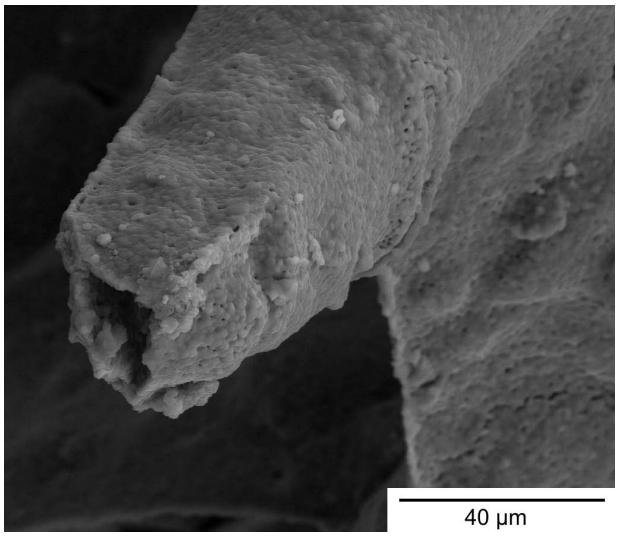


**Fig. 8:** SEM micrograph showing the nanopores and the interconnected porosity of the HA scaffold.

The XRD pattern of the HA scaffolds calcined at 1250 °C for 2 h is characterized by sharp peaks of HA phase with no secondary phases present, which indicates that the scaffolds are composed of pure HA phase, Fig. 9.

The mechanical properties of the scaffolds used in bone tissue engineering are an important issue. They should be maintained for sufficient time until the formed new bone can support itself; during the process of osteoblast growth, proliferation and differentiation. The studied scaffolds showed a crushing strength value of 0.82 ± 0.01 MPa and a bending strength of 1.72 ± 0.11 MPa. In agreement with Lorenzo *et al.* [33], we believe that pore area has the dominant influence on the mechanical properties of the obtained scaffolds.

Fig. 10 shows the mean value of Ca and P ions concentration (mg/L) as a function of the immersion time in the SBF. The results reveal that the Ca and P ion concentrations decreased considerably during the first week owing to the consumption of such ions in the formation of apatite on the surface of the scaffolds. From the second to the fourth week the decrease in the $Ca^{+2}$ and $P^{+3}$ ion concentration is nearly stable, which revealed that the maximum amount of apatite precipitate has deposited on the HA scaffold surface in the first week and transformed into stable bone-like apatite crystals. The thin-film XRD pattern of the HA/scaffold surface confirms the above-mentioned result, Fig. 11. The figure shows the deposition of a hydroxyapatite layer on the HA/scaffold surface. It shows that the deposited HA layer has a hexagonal structure with the main diffraction peaks at 25.9° (002), 31.8° (211), 32.2° (112), 32.9° (300), 34.0° (202) and 39.9° (130) [according to ICDD PDF- 00 – 009 – 0432].

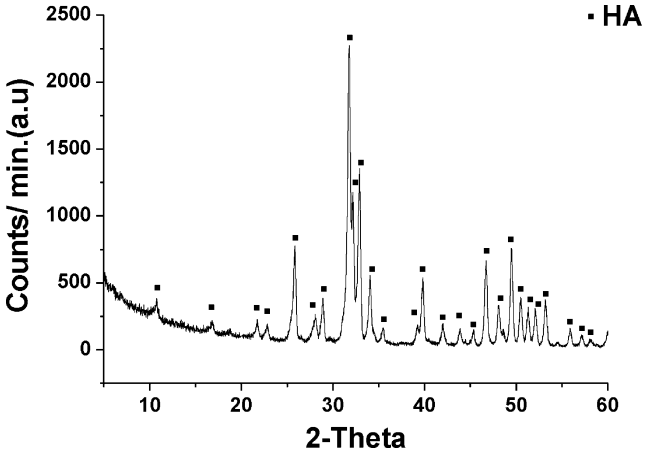


**Fig. 9:** XRD pattern of the HA scaffolds fired at 1250 °C for 2 h.

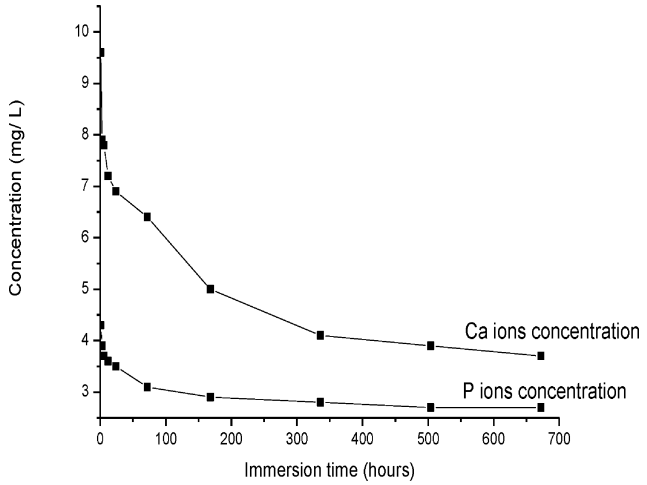


**Fig. 10:** Changes of Ca and P ions concentration as a function of incubation time periods in SBF.

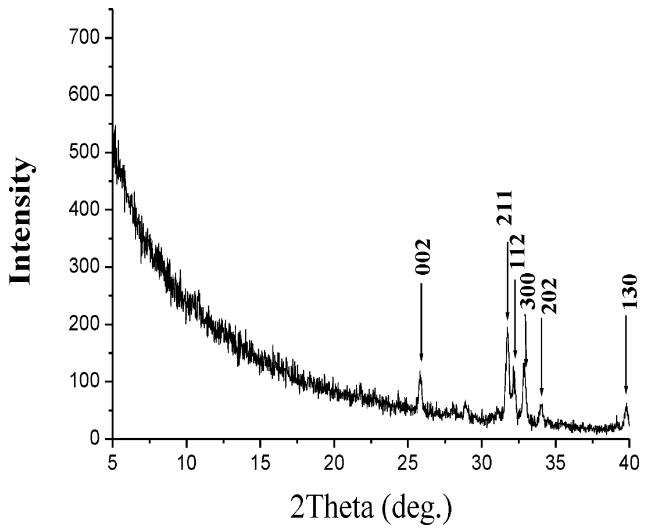


**Fig. 11:** Thin-film XRD pattern of the HA scaffold surface; immersed in SBF for 4 weeks.

The SEM micrograph of the HA scaffolds immersed in SBF for four weeks is shown in Fig. 12a. It could be seen that the surface of the scaffolds is completely covered with fine flake-shaped apatite grains. It demonstrates the good homogeneity distribution of the apatite particles on the scaffold surface. The SEM/EDS analysis of the indicated region is shown in Fig. 12b. The figure indicates the presence of $Ca^{+2}$ and $P^{+4}$ ions. The Ca/P ratio confirmed the formation of stoichiometric apatite (1.67).

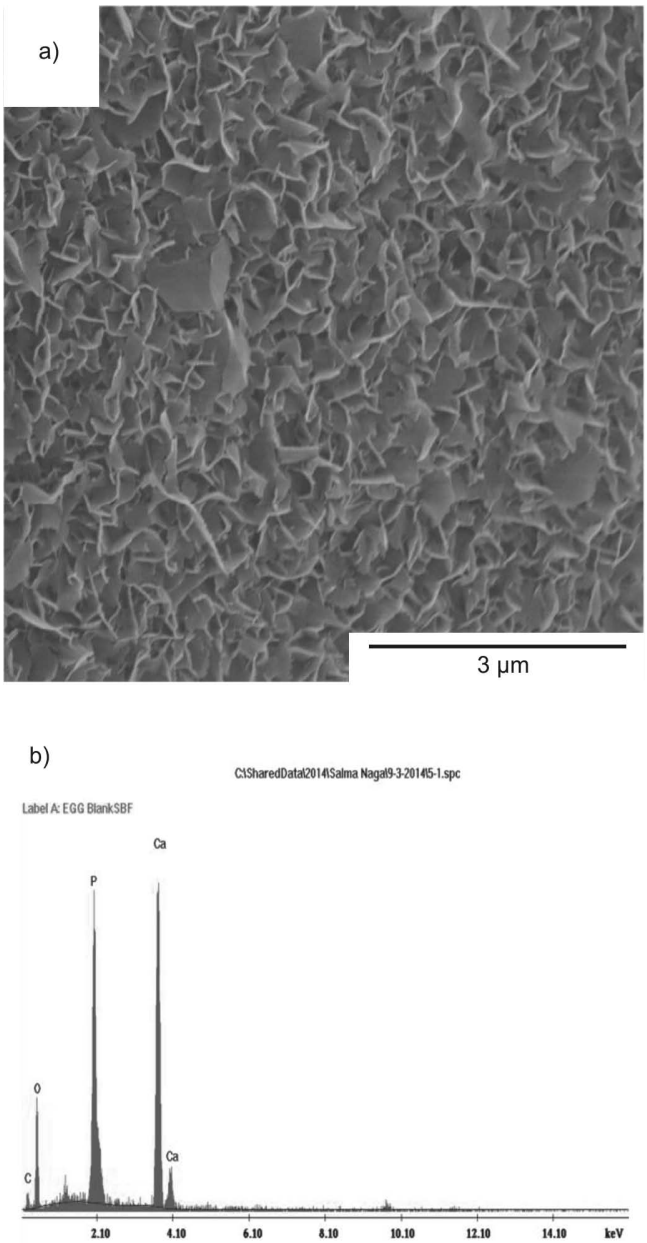


**Fig. 12:** SEM micrograph of the HA scaffold immersed in SBF for 4 weeks (a) and energy-dispersive XRD spectra (EDS) of immersed HA scaffold surfaces; immersed in SBF for 4 weeks (b).

## IV. Conclusions

1 Nano-sized hydroxyapatite powder with a grain size ranging between 35 and 122 nm was prepared from eggshells according to the indirect method.

2 The prepared powder is composed of HA, and it is stable up to 1100 °C.

3 The scaffolds calcined at 1250 °C for 2 h possess an appropriate architecture suitable to meet both the biological and mechanical requirements for scaffolds used in bone tissue engineering.

4 On the basis of the study results, it could be inferred that the prepared hydroxyapatite scaffolds synthesized from egg shells have great potential for use as an economical biomaterial.

## References

1 GLOBAL POULTRY TRENDS 2013 – Hen Egg Production in Africa and Oceania, The poultry site, www.thepoultrysite.com.

2 Rivera, E.M., Araiza, M., Brostow, W., Castăno, V.M., Diaz-Estrada, J.R., Hermández, R., Rodriguez, J.R.: Synthesis of hydroxyapatite from egg-shells, *Mater. Lett.*, **41**, 128 – 134, (1999).

3 Akram, M., Ahmed, R., Shakir, I., Ibrahim, W.A.W., Hussain, R.: Extracting hydroxyapatite and its precursors from natural resources, *J. Mater. Sci.*, **49**, [4], 1461 – 1475, (2014).

4 Siddharthan, A., Sampath Kumar, T.S., Seshadri. S.K.: Synthesis and characterization of nanocrystalline apatites from eggshells at different Ca/P ratios, *Biomed. Mater.*, **4**, 045010 – 045019, (2009).

5 Park, J.W., Bae, S.R., Suh, J.Y., Lee, D.H., Kim, S.H., Kim, H., Lee, C.S.: Evaluation of bone healing with eggshell-derived bone graft substitutes in rat calvaria, a pilot study, *J. Biomed. Mater. Res. A*, **87A**, 203 – 214, (2008).

6 Zhang, C.M., Yang, J., Quan, Z.W., Yang P.P., Li, C.X., Hou, Z.Y., Lin, J.: Hydroxyapatite nano- and microcrystals with multiform morphologies: controllable synthesis and luminescence properties, *Cryst. Growth Des.*, **9**, 2725 – 2733, (2009).

7 Wu, S.C., Tsou, H.K., Hsu, H.C., Hsu, S.K., Liou, S.P., Ho, W.F.: A hydrothermal synthesis of eggshell and fruit waste extract to produce nanosized hydroxyapatite, *Ceram. Int.*, **39**, 8183 – 8188, (2013).

8 Sanosh, K.P., Chu, M., Balakrishnan, A., Kim. T.N., Cho, S.: Utilization of biowaste eggshells to synthesize nanocrystalline hydroxyapatite powders, *Mater. Lett.*, **63**, 2100 – 2102, (2009).

9 Meski, S., Ziani, S., Khireddine, H.: Removal of lead ions by hydroxyapatite prepared from eggshell, *J. Chem. Eng. Data.*, **55**, 3923 – 3928, (2010).

10 Ho, W.F., Hsu, H.C., Hsu, S.K., Hung, C.W., Wu, S.C.: Calcium phosphate bioceramics synthesized from eggshell powders through a solid state reaction, *Ceram. Int.*, **39**, 6467 – 6473, (2013).

11 Chaudhuri, B., Mondal, B., Modak, D.K., Pramanik, K., Chaudhuri, B.K.: Preparation and characterization of nanocrystalline hydroxyapatite from eggshell and $K_2HPO_4$ solution, *Mater. Lett.*, **97**, 148 – 150, (2013).

12 Liu, J., Li, K., Wang, H., Zhu, M., Yan, H.: Rapid formation of hydroxyapatite nanostructures by microwave irradiation, *Chem. Phys. Lett.*, **396**, 429 – 432, (2004).

13 Martins, M.A., Antos, C.S., Almeida, M.M., Costa, M.E.U.: Hydroxyapatite micro and nano-particles: nucleation and growth mechanism in the presence of citrate species, *J. Colloid. Interf. Sci.*, **318**, 210 – 216, (2008).

14 Wang, Y., Hassan, M.S., Gunawan, P., Lau, R., Wang, X., Xu, R.: Polyelectrolyte mediated formation of hydroxyapatite microspheres of controlled size and hierarchical structure, *J. Colloid. Interf. Sci.*, **339**, 69 – 77, (2009).

15 Mondal, S., Bardhan, R., Mondal, B., Dey, A., Mukhopadhyay, S.S., Roy, S., Guha, R., Roy, K.: Synthesis, characterization and *in vitro* cytotoxicity assessment of hydroxyapatite from different bioresources for tissue engineering application, *B. Mater. Sci.*, **35**, [4], 683 – 691, (2012).

[16] Lee, S.J., Kwak, J.Y., Kriven, W.M.: Effect of a polymer addition on the crystallite size and sinterability of hydroxyapatite prepared with CaO powder and phosphoric acid, *J. Ceram. Process. Res.*, **13**, [3], 243 – 247, (2012).

[17] Lee, S.W., Balázsi, C., Balázsi, K., Seo, D.H., Kim, H.S., Kim, C.H., Kim, S.G.: Comparative study of hydroxyapatite prepared from seashells and eggshells as a bone graft material, *Tissue Eng. Regen. Med*., **11**, [2], 113 – 120, (2014).

[18] Adak, M.D., Chattopadhyaya, A.K., Purohit, K.M.: Synthesis of nano-crystalline hydroxyapatite from kitchen waste, *J. Pharm. Res*., **3**, [8], 1930 – 1932, (2010).

[19] Prabakaran, K., Rajeswari, S.: Spectroscopic investigations on the synthesis of nano- hydroxyapatite from calcined eggshell by hydrothermal method using cationic surfactant as template, *Spectrochim. Acta. A*, **74**, 1127 – 1134, (2009).

[20] Murphy, W.L., Dennis, R.G., Kileny, J.L., Mooney, D.J.: Salt fusion: an approach to improve pore interconnectivity within tissue engineering scaffolds, *Tissue Eng.*, **8**, 43 – 52, (2002).

[21] Whang, K., Thomas, C.H., Healy, K.E., Nuber, G.: A novel method to fabricate bioabsorbable scaffolds, *Polymer*, **36**, 837 – 842, (1995).

[22] Whang, K., Goldstick, T.K., Healy, K.E.: A biodegradable polymer scaffold for delivery of osteotropic factors, *Biomaterials*, **21**, 2545 – 2551, (2000).

[23] Kim, T.K., Yoon, J.J., Lee, D.S., Park, T.G.: Gas foamed open porous biodegradable polymeric microspheres, *Biomaterials*, **27**, 152 – 129, (2006).

[24] Rouholamin, D., Smith, P.J., Ghassemieh, E.: Control of morphological properties of porous biodegradable scaffolds processed by supercritical $CO_2$ foaming, *J. Mater. Sci.*, **48**, 3254 – 3263, (2013).

[25] Liulan, L., Huicun, Z., Li, Z., Qingxi, H., Minglum, F.: Design and preparation of bone tissue engineering scaffolds with porous controllable structure, *J. Wuhan Uni. Technol. Mater. Sci. Ed*., **24**, 174 – 180, (2009).

[26] Pujiang, S., Yubao, L., Li, Z.: Fabrication and characterization of n- HA/CS porous scaffolds containing ALC/CS microspheres, *J. Funct. Mater*., **37**, 1798 – 1800, (2006).

[27] Liulan, L., Ju, S., Cen, L., Zhang, H., Hu, Q.: Fabrication of porous β-TCP scaffolds by combination of rapid prototyping and freeze drying technology. 7th Asian- Pacific Conference on Medical Biological Engineering, IFMBE Proceedings, **19**, 88 – 91, (2008).

[28] Todea, M., Frentiu, B., Turcu, R.F.V., Berce, P., Simon, S.: Surface structure changes on aluminosilicate microspheres at the interface with simulated body fluid, *Corros. Sci.*, **54**, 299 – 306, (2012).

[29] Prabakaran, K., Balamurugan, A., Rajeswari, S.: Development of calcium phosphate based apatite from hen's eggshell, *B. Mater. Sci*., **28**, [2], 115 – 119, (2005).

[30] Hui, P., Meena, S.L., Singh, G., Agarawal, R.D., Prakashe. S.: Synthesis of hydroxyapatite bio-ceramic powder by hydrothermal method, *J. Miner. Mater. Charact. Eng.*, **9**, [8], 683 – 692, (2010).

[31] Gergely, G., Wéber, F., Lukács, I., Illés, L., Tóth, A.L., Horváth, Z.E., Mihály, J., Balázsi, C.: Nano-hydroxyapatite preparation from biogenic raw materials, *Cent. Eur. J. Chem.*, **8**, [2], 375 – 381, (2010).

[32] Kim, B.S., Mooney, D.J.: Development of biocompatible synthetic extracellular matrices for tissue engineering, *Trends Biotechnol*., **16**, 224 – 230, (1998).

[33] Lorenzo, L.M.R., Regí, M.V., Ferreira J.M.F.: Fabrication of hydroxyapatite bodies by uniaxial pressing from a precipitated powder, *Biomaterials*, **22**, 583 – 588, (2001).